Astronomy & Astrophysics manuscript no. language˙edited
December 22, 2010

The subgiant branch of ω Cen seen through high-resolution spectroscopy. I. The first stellar generation in ω Centauri?⋆

E. Pancino[1], A. Mucciarelli[2], L. Sbordone[3,4], M. Bellazzini[1], L. Pasquini[5], L. Monaco[6], F. R. Ferraro[2]

[1] INAF-Osservatorio Astronomico di Bologna, via Ranzani 1, I-40127, Bologna, Italy
e-mail: elena.pancino@oabo.inaf.it
[2] Dipartimento di Astronomia, Università degli studi di Bologna, via Ranzani 1, I-40127, Bologna, Italy
[3] Max Planck Institute for Astrophysics, Karl-Schwarzschild-Str. 1, D-85741 Garching, Germany
[4] Laboratoire d'Etudes des Galaxies, Etoiles, Physique et Instrumentation GEPI, Observatoire de Paris, Avenue de L'Observatoire 61, F-75014, France
[5] European Southern Observatory, Karl-Schwarzschild-Strasse 2, D-85748 Garching bei München, Germany
[6] European Southern Observatory, Casilla 19100, Santiago, Chile

Received September XX, XXXX; accepted March XX, XXXX

ABSTRACT

We analysed high-resolution UVES spectra of six stars belonging to the subgiant branch of ω Centauri, and derived abundance ratios of 19 chemical elements (namely Al, Ba, C, Ca, Co, Cr, Cu, Fe, La, Mg, Mn, N, Na, Ni, Sc, Si, Sr, Ti, and Y). A comparison with previous abundance determinations for red giants provided remarkable agreement and allowed us to identify the sub-populations to which our targets belong. We found that three targets belong to a low-metallicity population at [Fe/H]≃–2.0 dex, [α/Fe]≃+0.4 dex and [s/Fe]≃0 dex. Stars with similar characteristics were found in small amounts by past surveys of red giants. We discuss the possibility that they belong to a separate sub-population that we name VMP (very metal-poor, at most 5% of the total cluster population), which – in the self-enrichment hypothesis – is the best-candidate first stellar generation in ω Cen. Two of the remaining targets belong to the dominant metal-poor population (MP) at [Fe/H]≃–1.7 dex, and the last one to the metal-intermediate (MInt) one at [Fe/H]≃–1.2 dex. The existence of the newly defined VMP population could help to understand some puzzling results based on low-resolution spectroscopy (Sollima et al., Villanova et al.) in their age differences determinations, because the metallicity resolution of these studies was probably not enough to detect the VMP population. The VMP could also correspond to some of the additional substructures of the subgiant-branch region found in the latest HST photometry (Bellini et al.). After trying to correlate chemical abundances with substructures in the subgiant branch of ω Cen, we found that the age difference between the VMP and MP populations should be small (0±2 Gyr), while the difference between the MP and MInt populations could be slightly larger (2±2 Gyr).

Key words. stars: abundances – stars: main sequence –globular clusters: individual (ω Centauri); NGC 6397

1. Introduction

Much has been written on ω Cen, which is probably the most studied cluster in the Milky Way (van Leeuwen et al., 2002). From the pioneering studies in the 60s to the latest high-quality data and models, more and more details of its multiple stellar populations have come to light, but the picture did not become as clear as expected. Excellent photometries and astrometric catalogues have recently been produced by both ground-based (such as Lee et al., 1999; Pancino et al., 2000; van Leeuwen et al., 2000; Hilker & Richtler, 2000; Hughes & Wallerstein, 2000; Sollima et al., 2005a; Calamida et al., 2009; Bellini et al., 2009) and space telescopes (e.g., Ferraro et al., 2004; Bedin et al., 2004; Bellini et al., 2010), complemented by high-quality spectroscopic abundance studies both at high (e.g., Norris & Da Costa, 1995; Smith et al., 2000; Cunha et al., 2002; Pancino, 2003; Johnson et al., 2008, 2009; Johnson & Pilachowski, 2010; Marino et al., 2010) and low (Norris et al., 1996; Suntzeff & Kraft, 1996; Sollima et al., 2005b; Stanford et al., 2006; Villanova et al., 2007) resolution. Nevertheless, several puzzles still await solutions.

One of the open problems concerns the most sensitive region of the colour magnitude diagram (hereafter CMD) to age differences: the subgiant branch (SGB). A large number of photometric and low-resolution spectroscopic studies (Hughes & Wallerstein, 2000; Hilker & Richtler, 2000; Pancino, 2003; Hughes et al., 2004; Hilker et al., 2004; Rey et al., 2004; Ferraro et al., 2004; Stanford et al., 2006) found age spreads ranging from 2 to 6 Gyr, with a few exceptions and puzzles (see Section 5.3, for more details). One example of the difficulties encountered in the study of this complex region is posed by the two studies by Sollima et al. (2005b) and Villanova et al. (2007), who used the same ACS dataset and low-resolution spectra of similar quality, but reached opposite conclusions on the total age spread – and age distribution – of ω Cen. Still, even with the best ACS photometries (see, e.g. Bellini et al., 2010), it is not easy to understand which features of the SGB region correspond to each of the populations that are spectroscopically identified on the red giant branch (RGB), which are known in great detail thanks to the above cited works. This understanding is crucial to solve the relative ages problem in ω Cen, and to derive the age-metallicity relation, a fundamental ingredient of any model for the formation and evolution of this unique stellar system.

⋆ Based on data collected at the ESO VLT in Chile, with UVES and FLAMES under programs 68.D-0332(A) and 079.D-0021. Also based on literature data from the ESO WFI, under programs 62.L-0354 and 63.L-0439, and on data collected from the following online databases: NIST, VALD, Kurucz, GEISA.

Table 1. Observing Logs.

ID_{WFI}	R.A. (J2000) (deg)	Dec (J2000) (deg)	V (mag)	$(B-V)_0$ (mag)	$(V-I)_0$ (mag)	R $(\lambda/\delta\lambda)$	$t_{exp}^{(tot)}$ (sec)	S/N (@550nm)	V_r (km s^{-1})	Notes
503358	201.960086	-47.759426	17.53	0.65	0.65	45 000	10800	50	231.0 ± 0.2	Lower SGB
503951	201.870201	-47.746107	17.58	0.65	0.65	45 000	11400	50	235.8 ± 0.1	Lower SGB
507109	201.848173	-47.692322	17.31	0.60	0.66	45 000	11288	50	229.7 ± 0.5	Upper SGB
507633	201.813303	-47.685166	17.39	0.56	0.66	45 000	12000	45	226.7 ± 0.3	Upper SGB
512115	201.846338	-47.637524	17.64	0.65	0.66	45 000	11400	45	241.4 ± 0.1	Lower SGB
512938	201.804070	-47.630694	17.32	0.60	0.65	45 000	10000	50	234.6 ± 0.2	Upper SGB

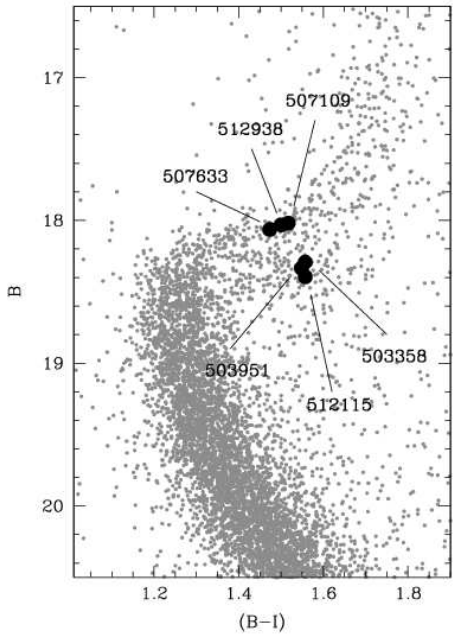

Fig. 1. Location of the programme stars on the CMD of ω Cen. The WFI B, B–I photometry of stars in CCD#5 (from Pancino et al., 2000) is shown as grey dots. The six UVES targets are marked (black filled circles) with their WFI catalogue numbers.

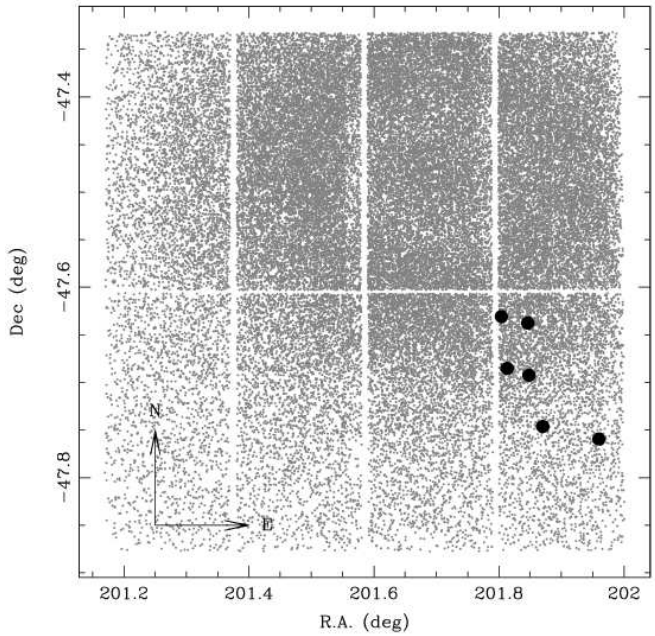

Fig. 2. Location of the programme stars on the area of ω Cen. Grey dots mark stars belonging to the WFI photometry by Pancino et al. (2000). Filled circles mark the postion of the six UVES targets.

In this paper we present the analysis of a set of UVES high-resolution spectra of six SGB stars, selected from the wide field photometric catalogue by Pancino et al. (2000) and Pancino (2003). A preliminary analysis of the same dataset was presented by Pancino (2003). We describe the spectra reductions in Section 2; the abundance analysis in Section 3; and the abundance ratio results in Section 4. Our main results are discussed in detail in Section 5 and are summarized in Section 6.

2. Observations and data reduction

We selected our six targets from the WFI B and I photometry presented in Pancino et al. (2000), complemented with V magnitudes from Pancino (2003). The coordinates were obtained using the astrometric catalogue by van Leeuwen et al. (2000). As shown in Figures 1 and 2, the SGB region of ω Cen in the external parts of the cluster shows clear substructures (all our targets lie on the WFI CCD#5). This is more clearly seen in other literature photometries (Ferraro et al., 2004; Bedin et al., 2004; Bellini et al., 2010), but they are obtained from space, with the HST, in the very centre of ω Cen, where UVES follow-up from the ground would be difficult. Three of the programme stars were selected towards the upper envelope of the SGB and another three towards the lower envelope.

Echelle spectroscopy was obtained on 18–20 March 2002, with UVES at the ESO Kueyen (VLT UT2) telescope, on Cerro Paranal, Chile. Table 1 reports the log of the observations, along with some basic target information. Each star was observed twice and on different nights, both to minimize the cosmic rays impact and to identify possible radial velocity shifts. Given the faint magnitude of these stars (V≃17.5), the spectra were binned on chip (2×1), so that the resolution element is covered by ≃3 pixels. A final S/N≃50 per pixel was achieved around 550 nm.

The red spectra (upper and lower red CCDs) were reduced with the ESO-UVES pipeline (Ballester et al., 2000), which semi-automatically performs bias correction, flat-field correction, inter-order background subtraction, optimal extraction with cosmic-ray rejection, wavelength calibration (with rebinning), and final merging of all overlapping orders. However, since the

Table 2. Equivalent widths and atomic data for the lines used in the classical abundance analysis of the program stars. The complete version of the table is available at CDS. Here we show a few lines to illustrate its contents.

				Star WFI 503358			Star WFI 503951				Star WFI 512115			Star WFI 512938		
λ	El	χ_{ex}	$\log gf$	EW	δEW	Q	EW	δEW	Q	...	EW	δEW	Q	EW	δEW	Q
(Å)		(eV)	(dex)	(mÅ)	(mÅ)		(mÅ)	(mÅ)			(mÅ)	(mÅ)		(mÅ)	(mÅ)	
4283.01	CaI	1.89	-0.29	77.0	8.9	1.463	95.5	12.2	1.832	...	0.0	0.0	0.000	67.0	5.6	1.248
4289.37	CaI	1.88	-0.39	75.6	8.0	1.566	80.2	7.3	1.378	...	79.7	12.7	1.492	64.5	6.5	1.213
4298.99	CaI	1.89	-0.51	0.0	0.0	0.000	0.0	0.0	0.000	...	0.0	0.0	0.000	0.0	0.0	0.000
4302.53	CaI	1.90	0.18	0.0	0.0	0.000	0.0	0.0	0.000	...	0.0	0.0	0.000	0.0	0.0	0.000
4318.65	CaI	1.90	-0.29	72.8	8.1	1.876	93.6	7.5	1.747	...	0.0	0.0	0.000	61.1	3.7	0.851
4434.96	CaI	1.89	0.07	0.0	0.0	0.000	0.0	0.0	0.000	...	0.0	0.0	0.000	81.0	5.9	1.227

S/N ratio is significantly lower on the blue part of the spectra (S/N≃25 around 450 nm), we decided to manually perform the echelle reduction for the blue CCD with the *noao.imred.ccdred* and *noao.imred.echelle* packages within IRAF[1].

The two one-dimensional and wavelength-calibrated spectra obtained for each star were normalized by fitting their continua with a cubic spline, then corrected for the main telluric absorption features (*noao.onedspec.telluric* in IRAF), using as a reference a hot, fast rotating star (HR 5206/HD 120640) selected from the *Bright Star Catalog* (Hoffleit & Jaschek, 1991), and observed each night at an airmass not too different from the targets. Finally the spectra were summed – after correcting for radial velocity shifts – to produce one single spectrum for each of the six observed stars.

Radial velocities were obtained with DAOSPEC[2] (Stetson & Pancino, 2008) and the procedure described by Pancino et al. (2010). In short, the laboratory wavelength of selected absorption lines (Section 3.1) was used to measure the observed radial velocity. The heliocentric correction was computed with IRAF and the telluric H_2O and O_2 absorption bands redward of 580 nm were used to correct for zeropoint shifts. All six stars were radial velocity members of ω Cen, considering an average V_r=232.8 or 233.4 km s^{-1}, as determined by Meylan et al. (1995) and Pancino et al. (2007), respectively, with a central velocity dispersion of the order of 20 km s^{-1}. The resulting velocities and errors are listed in Table 1.

3. Abundance analysis

3.1. Equivalent widths and atomic data

We selected the majority of our lines and of their atomic data from the VALD[3] database (Kupka et al., 1999). To identify reliable lines, high S/N median spectra of the six UVES targets were created and the cleanest, unblended lines of the available elements were identified. Only lines that appeared in at least three of the six stars were retained in our preliminary selection. DAOSPEC was used to measure the equivalenth widths (EW) of all the chosen lines. A first-pass abundance analysis was performed (Section 3.3): lines that showed systematically higher errors and bad Q parameters (see Stetson & Pancino, 2008; Pancino et al., 2010, for details) and that simultaneously gave systematically discrepant abundances were rejected. Finally, all lines that gave EW<15 mÅ, or EW>100 mÅ (with a few exceptions, see Section 3.3) were not used to determine abundances. The DAOSPEC EW measurements used for the abundance analysis are shown in Table 2, along with the formal error δEW and the quality parameter Q for each line (Stetson & Pancino, 2008).

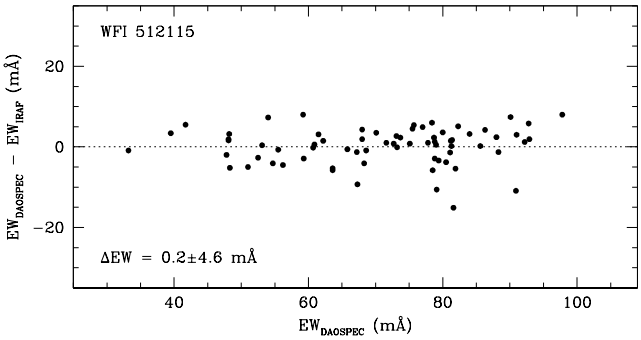

Fig. 3. Comparison between DAOSPEC and IRAF *splot* measurements for star WFI 512115.

A few lines were measured with the help of spectral synthesis because they were reported to have significant hyperfine structure (HFS). In particular, we used the atomic data by Martin et al. (1988) for the Mn I lines at 4030, 4033, 4034, 4041, and 4055 Å; the NIST[4] atomic data for the Ba II lines at 4934, 5853, 6141, and 6496 Å; the atomic data by Lawler et al. (2001) for the La II lines at 3988, 4086, 4123, and 4238 Å; and the atomic data by Bielski (1975) for the 5105 Å Cu I line[5]. For the CH and CN molecular bands, we used the Kurucz molecular linelists[6], but we had to revise the loggf values of C downwards by 0.3 dex, similarly to what was reported by Bonifacio et al. (1998), Lucatello et al. (2003), and Spite et al. (2005) (see also Section 3.3).

3.2. Atmospheric parameters and best-model search

A first guess of the atmospheric parameters was derived from the WFI photometry. Dereddened $(B–V)_0$ and $(V–I)_0$ colours were obtained from B, V, and I magnitudes adopting E(B–V)=0.11 (Lub, 2002) and E(V–I)/E(B–V)=1.30 (Dean et al., 1978), and are listed in Table 1 along with the V magnitudes. The V–I colour was converted from the original V–I_C, based on the Cousins I magnitude, to the V–I_J, based on the Johnsons I magnitude, with

[1] http://iraf.noao.edu/. IRAF is distributed by the National Optical Astonomy Observatories, which is operated by the association of Universities for Research in Astronomy, Inc., under contract with the National Science Foundation.

[2] http://www3.cadc-ccda.hia-iha.nrc-cnrc.gc.ca/community/STETSON/daospec/ ; http://www.bo.astro.it/~pancino/projects/daospec.html

[3] http://www.astro.uu.se/~vald/

[4] http://physics.nist.gov/PhysRefData/ASD/index.html

[5] We could not use the 5872 Å Cu I line since it falls into the gap between the two UVES red CCDs.

[6] http://kurucz.harvard.edu/LINELISTS/LINESMOL/

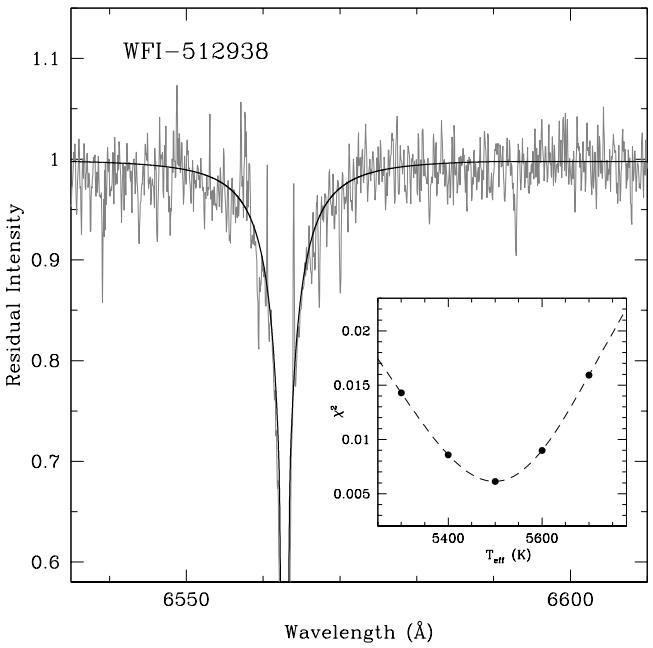

Fig. 4. Example of the H_α profile fit for star WFI 512938. The solid line represents the best-fitting synthetic spectrum where all parameters are kept fixed as in Table 3 except for the effective temperature, T_{eff}. The inset panel shows the run of the χ^2 of fits with different values of T_{eff}.

the relations by Bessell (1979). Effective temperatures (hereafter T_{eff}) and bolometric corrections (BC_V) were obtained with the Alonso et al. (1999) calibration. Surface gravities (hereafter $\log g$) were then derived by means of fundamental relations:

$$\log g_* = 0.4(M_V + BC_V) + 4\log T_{eff,*} - 12.61, \quad (1)$$

where the solar values where assumed in conformity with the IAU recommendations (Andersen, 1999), i.e., $\log g_\odot = 4.437$, $T_{eff,\odot}$=5770 K and $M_{bol,\odot}$=4.75. A typical mass of 0.8 $M_\odot$ was assumed for the programme stars (Bergbusch & VandenBerg, 2001), and we used $(m–M)_V$=14.04±0.11 mag (Bellazzini et al., 2004). An independent estimate of T_{eff}, which is the most influential parameter when determining abundances, was also derived from the profile fitting of the H_α line wings. We computed Kurucz atmosphere models with ATLAS9 (Kurucz, 1993, 2005), using gravities and global metallicities close to the photometric parameters of each target. We built synthetic spectra with a modified version of SYNTHE[7], exported for the Linux OS (Sbordone et al., 2004). An example of a typical H_α profile fit is shown in Figure 4.

We found general agreement between the photometric and the H_α T_{eff} estimates, but the scatter was large, with differences of up to 300 K in some cases. When averaging estimates from B–V and V–I together, the scatter went down (see Table 3). We decided to rely on the H_α temperatures as a first guess for the spectroscopic analysis. First guess $\log g$ values were derived from H_α temperatures using V magnitudes and the Alonso et al. (1999) calibration.

The final atmospheric parameters were then derived through the usual "spectroscopic method" (see Section 3.3 for abundance calculation details): after we had a good number of Fe I and Fe II lines (approximately 200 and 10, respectively, depending on the star), we re-adjusted the parameters by choosing those that minimized *(i)* the slope of [Fe I/H] versus the excitation potential, χ_{ex}; *(ii)* the slope of [Fe I/H] versus the EW of each line[8]; *(iii)* the difference between the average [Fe I/H] and [Fe II/H]; and finally by checking that [Fe I/H] did not change significantly with wavelength. The adopted atmospheric parameters are listed in Table 3 along with the photometric and H_α temperatures, for comparison. We found that, on average, spectroscopic T_{eff} estimates based on Fe were lower than H_α ones by 17±52 K, and also lower than photometric ones by 83±26 K.

Table 3. Atmospheric model parameters.

ID_{WFI}	$T_{eff}^{(phot)}$ (K)	$T_{eff}^{(H_\alpha)}$ (K)	$T_{eff}^{(Fe)}$ (K)	$\log g^{(Fe)}$ (dex)	$v_t^{(Fe)}$ (km s^{-1})	[M/H] (dex)
503358	5600	5550	5500	3.6	1.2	–1.5
503951	5600	5500	5500	3.6	1.2	–1.5
507109	5600	5600	5500	3.4	1.3	–2.0
507633	5700	5650	5650	3.4	1.1	–2.0
512115	5600	5500	5500	3.7	1.2	–1.0
512938	5600	5500	5550	3.2	1.4	–2.0

3.3. Abundance calculations

For most chemical species we computed abundances with the help of the updated version of the original code by Spite (1967). Our reference solar abundance was that of Grevesse et al. (1996). Once the best set of atmospheric parameters was chosen for each star (see Section 3.2), we used the new MARCS[9] model atmospheres with standard composition[10]. We chose the closest available global model metallicity (taking into account α-enhancement) of the ω Cen sub-populations, as reported in Table 3.

For all species we computed a $3\,\sigma$-clipped average of abundances resulting from each line. For elements that had both neutral and ionized lines, we computed the weighted (on the number of lines) average of the two ionization stages to obtain [El/Fe]. We typically rejected lines that had EW>100 mÅ, where the Gaussian approximation could fail, or EW<15 mÅ, since the relative error was too high. For elements with few lines, and where we had to rely mostly on strong lines, we either performed spectral synthesis, or checked that the DAOSPEC measurements were not too underestimated by visually inspecting the spectrum and overlaying the DAOSPEC Gaussian fit on each strong line.

A few element abundances (Mn, Cu, Ba, and La) were derived with the help of spectral synthesis, taking into account HFS of single lines when needed (see also Section 3.1). We used the MOOG[11] (Sneden, 1973) package in combination with the "best MARCS models" above to find the best fitting spectrum[12]. All

[7] The broadening theory adopted in this routine is that of Ali & Griem (1965) and Vidal et al. (1973).

[8] We adopt the observed EW rather than the theoretical one ($\log gf - \theta\chi_{ex}$, Magain, 1984), following the discussion by Mucciarelli (2010).

[9] http://marcs.astro.uu.se/

[10] This means [α/Fe]=+0.4 for metal-poor stars of [Fe/H]<–1.0 and reaching [α/Fe]=0 at [Fe/H]=0, following schematically the typical halo-disk behaviour of the Milky Way field population.

[11] http://verdi.as.utexas.edu/moog.html

[12] To quantify the uncertainty related to the use of two different codes, one for the EW analysis and the other for spectral synthesis, we re-

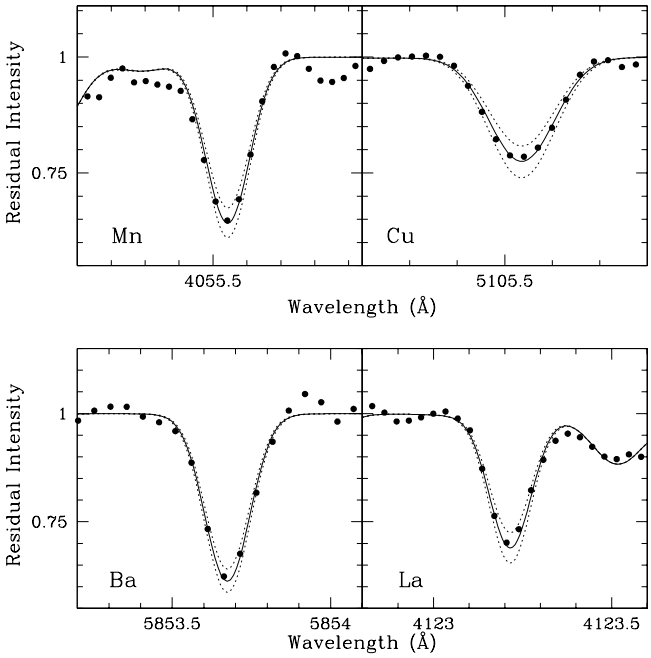

Fig. 5. Examples of spectral synthesis applied to single lines for star WFI 512115. Big dots are the observed spectrum, solid lines represent the best fitting synthetic spectra, computed with all parameters fixed to the values of Tables 3 and 4, except for the abundance of the element under consideration. Spectra computed with the line abundances altered by ±0.1 dex – with respect to the best fitting spectrum – are shown as dotted lines.

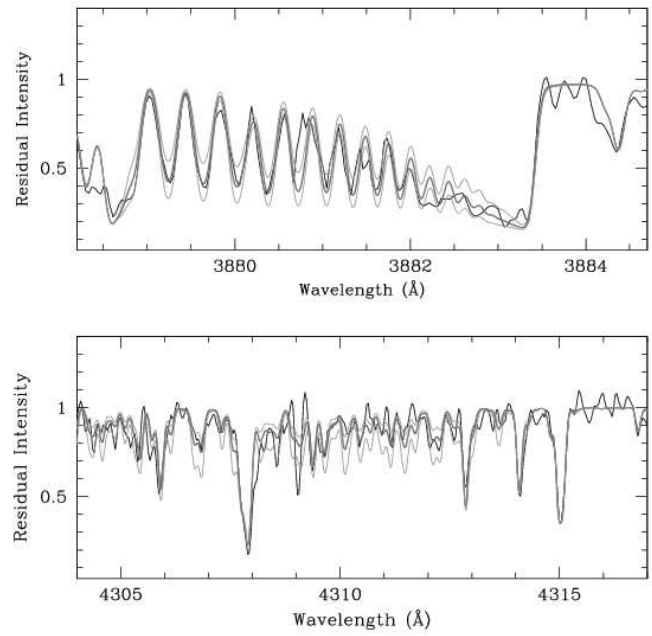

Fig. 6. Examples of spectral synthesis applied to the CN (top panel) and CH (bottom panel) molecular bands. Solid black curves represent the observed spectra for star WFI 512115, thick grey curves represent the best fitting synthetic spectra, while thin grey lines represent synthetic spectra differing from the best fit by ±0.2 dex in the N (top panel) and C (bottom panel) abundances.

atmospheric parameters and the abundances of other blended elements (when present) were kept fixed and only the abundance of the element of interest was changed until the residuals of the fit were minimized. C and N abundances were derived by spectral synthesis of the molecular CN and CH bands at 3880 Å and 4300 Å, respectively. Examples of line fits with spectral synthesis are shown in Figures 5 and 6.

More in detail, carbon and nitrogen abundances were measured by minimizing the residuals between grids of synthetic spectra and the observed ones around the CN and CH bands. In particular, C abundances were derived by fitting the CH G-band between 4300 and 4340 Å, including the band heads of the (0-0), (1-1) and (2-2) bands of the $A^2\Delta$–$X^2\Pi$ CH transitions; N abundances were derived with the CN $B^2\Sigma^+$–$X^2\Sigma^+$ (0,0) UV band at 3870-3890 Å. In the measurement process, we kept the atmospheric parameters and all the atomic abundances fixed to the values of Tables 3 and 4, and we used the molecular data from the Kurucz database although, as discussed in Section 3.1, a correction of –0.3 dex to the loggf values of C was necessary. For each star, we computed synthetic spectra around the G-band by changing the C abundance only, and once the best fit was found, we employed the found C abundance in the fit of the CN band, where we changed only the N abundance. The procedure was then iterated a few times, repeating the fit for the CH band with the newly found N abundance, until the variations in both C and N were well below 0.1 dex.

The abundance calculation results are reported in Table 4, and are discussed in Section 4.

3.4. Abundance uncertainties

We estimated the internal, random uncertainty caused by imperfections in the EW measurement (or spectral synthesis process) and in the line atomic data, as $\sigma/\sqrt{n}$, for those elements that had at least two surviving lines after a $3\,\sigma$-clipping pass. For elements that relied on one line only, including those analysed with spectral synthesis, we derived a typical uncertainty of 0.05 dex by means of the Cayrel (1988) approximated formula, and we indicated this typical uncertainty between parenthesis in Table 4.

The uncertainty owing to the continuum normalization procedure can be estimated from the average spread of the residual spectrum of each star after lines removal, which is automatically computed by DAOSPEC. For our spectra, this was ∼1%. According to Figure 2 by Stetson & Pancino (2008), this propagates to an approximate uncertainty in the EW estimates of ±3 mÅ, and finally in an uncertainty of the order of 0.05 dex in the derived abundances.

Another factor that has a big impact on the abundance ratios is the choice of atmospheric parameters (Section 3.2). As discussed by Cayrel et al. (2004), T_{eff}, log g and v_t are not strictly independent parameters when determined with the method of Section 3.3. Therefore, the best way to estimate the impact of the parameters' choice on abundance ratios is to change the most influential parameter, T_{eff}, and to re-optimize the other parameters that naturally re-adjust to accommodate the temperature change. The difference between abundances calculated with the "best model" and with the altered one is a robust estimate of the systematic uncertainty owing to the choice of stellar parameters.

analysed star WFI 507633 with MOOG, using the same linelist, EW, atomic data, atmospheric parameters and MARCS models. We found [Fe/H]=–2.02±0.02 which is well compatible with the abundance obtained with the Spite code (Table 4).

Table 4. Abundance ratios with random uncertainties (see text).

Element	WFI 503358 (dex)	WFI 503951 (dex)	WFI 507109 (dex)	WFI 507633 (dex)	WFI 512115 (dex)	WFI 512938 (dex)
[FeI/H]	–1.70±0.01	–1.58±0.01	–1.99±0.02	–2.05±0.02	–1.18±0.01	–2.03±0.02
[FeII/H]	–1.70±0.12	–1.56±0.09	–1.95±0.07	–1.94±0.05	–1.34±0.05	–1.99±0.10
[Fe/H]	–1.70±0.01	–1.58±0.01	–1.98±0.02	–2.04±0.02	–1.19±0.01	–2.03±0.02
[Al/Fe]	+0.13±(0.05)	+0.40±0.29	–0.12±(0.05)	+0.14±0.50	+0.80±0.05	–0.19±(0.05)
[Ba/Fe]	+0.57±0.12	+1.10±0.24	–0.06±0.24	–0.20±0.16	+0.64±0.12	–0.33±0.23
[C/Fe]	–0.02±0.15	–0.64±0.15	+0.07±0.15	–0.17±0.15	–0.94±0.15	–0.19±0.15
[Ca/Fe]	+0.40±0.03	+0.44±0.03	+0.32±0.05	+0.33±0.04	+0.43±0.08	+0.34±0.03
[Co/Fe]	–0.03±0.19	+0.21±0.12	–0.14±0.24	+0.08±0.06	+0.37±0.17	–0.06±0.12
[Cr/Fe]	+0.08±0.23	–0.08±0.06	–0.04±0.21	–0.15±0.10	+0.08±0.04	+0.03±0.17
[Cu/Fe]	–0.84±(0.05)	–0.60±(0.05)	<–0.93±(0.05)	<–0.47±(0.05)	–0.70±(0.05)	<–0.48±(0.05)
[La/Fe]	+0.24±0.06	+0.59±0.05	+0.12±0.08	–0.13±0.10	+0.18±0.09	–0.06±0.08
[Mg/Fe]	+0.46±0.11	+0.41±0.02	+0.35±0.06	+0.45±0.08	+0.41±(0.05)	+0.55±0.10
[Mn/Fe]	–0.78±0.13	–0.81±0.08	–0.60±0.11	–0.41±0.03	–0.61±0.03	–0.54±0.11
[N/Fe]	–0.12±0.30	+1.36±0.15	+0.57±0.20	+1.23±0.15	+1.26±0.25	–0.29±0.30
[Na/Fe]	+0.07±0.11	+0.60±0.12	+0.30±0.03	–0.15±0.33	+0.67±0.19	–0.42±0.37
[Ni/Fe]	–0.10±0.03	–0.03±0.04	+0.06±0.06	+0.03±0.09	–0.02±0.04	+0.13±0.08
[Sc/Fe]	–0.03±0.07	+0.20±0.05	+0.10±0.12	–0.07±0.09	–0.04±0.12	+0.18±0.14
[Si/Fe]	+0.38±0.14	+0.46±0.30	+0.27±(0.05)	+0.19±(0.05)	+0.35±0.39	+0.61±(0.05)
[Sr/Fe]	+0.38±0.04	+0.49±0.05	–0.13±0.11	–0.12±0.09	+0.25±0.12	–0.10±0.09
[Ti/Fe]	+0.25±0.04	+0.38±0.03	+0.30±0.04	+0.33±0.06	+0.38±0.04	+0.24±0.03
[Y/Fe]	+0.58±0.08	+0.71±0.06	+0.31±0.05	...	+0.69±0.13	+0.28±0.72

Table 5. Uncertanties owing to the choice of stellar parameters.

Element	WFI 512115 (T=5350)	WFI 507633 (T=5650)	UVES Average
[FeI/H]	±0.07	±0.05	±0.06
[FeII/H]	±0.05	±0.08	±0.07
[Al/Fe]	±0.02	±0.02	±0.02
[Ba/Fe]	±0.04	±0.06	±0.05
[Ca/Fe]	±0.03	±0.04	±0.04
[C/Fe]	±0.15	±0.15	±0.15
[Co/Fe]	±0.03	±0.02	±0.03
[Cr/Fe]	±0.17	±0.04	±0.11
[La/Fe]	±0.05	±0.05	±0.05
[Mg/Fe]	±0.05	±0.02	±0.04
[Mn/Fe]	±0.03	±0.02	±0.03
[N/Fe]	±0.20	±0.20	±0.20
[Na/Fe]	±0.01	±0.02	±0.02
[Ni/Fe]	±0.02	±0.01	±0.02
[Sc/Fe]	±0.06	±0.06	±0.06
[Si/Fe]	±0.02	±0.02	±0.02
[Sr/Fe]	±0.09	±0.15	±0.12
[Ti/Fe]	±0.02	±0.05	±0.04
[Y/Fe]	±0.05	±0.06	±0.06

We therefore chose our warmest and coolest stars and re-computed their abundances with models having T_{eff} altered by ±100 K, re-optimizing the other parameters according to the method described in Section 3.3. The final uncertainties are obtained by averaging the absolute abundance differences of the +100 and –100 altered models, and are reported in Table 5.

The global uncertainty (shown in all Figures from 8 to 13) is computed as the sum in quadrature of the random errors, the uncertainty owing to the continuum placement and the one owing to the choice of atmospheric parameters.

Table 6. Comparative analysis of NGC 6397.

Star	T_{eff} (K)	log$g$ (dex)	v_t (km/s)	Δ[Fe/H][a] (dex)	Notes
699	5500	3.4	1.3	+0.00	Gratton et al. (2001)
	5400	3.3	1.8	–0.10	Korn et al. (2007)
793	5500	3.4	1.3	–0.05	Gratton et al. (2001)
	5500	3.4	1.6	+0.06	Korn et al. (2007)
206810	5500	3.4	1.3	+0.09	Gratton et al. (2001)
	5500	3.4	1.8	+0.07	Korn et al. (2007)

[a]Differences in the sense: ours minus literature, with same parameters.

3.5. A comparison with NGC 6397

Usually, to test the goodness of an abundance analysis, a comparison with the Sun or Arcturus is performed. In our case, because our linelist was optimized for metal-poor subgiants, we would be performing an abundance analysis of the Sun relying only on strong lines, with EW>100 mÅ. These strong lines are rejected when analysing our UVES metal-poor stars, because at this resolution they start to significantly deviate from the Gaussian shape (see Figure 7 by Stetson & Pancino, 2008).

Therefore, while the general method was already tested on the Sun by Pancino et al. (2010), we preferred to compare our present results to another well studied cluster, such as NGC 6397. We downloaded UVES archive spectra of three subgiants (stars 206810, 669, and 793) in NGC 6397, published by Gratton et al. (2001) and later re-analysed by Korn et al. (2007), which have similar temperatures, gravities, and metallicities as the three most metal-poor SGB stars in our sample. We re-analysed them adopting the same parameters as Gratton et al. (2001) and as Korn et al. (2007), respectively, as detailed in Table 6. Obviously, the differences in the resulting [Fe/H] are

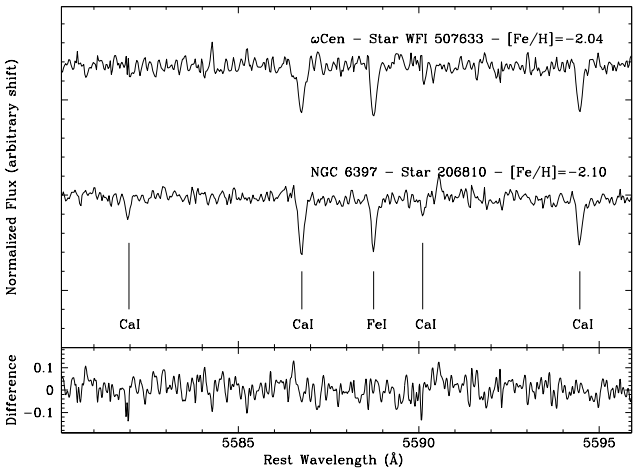

Fig. 7. Comparison between the spectra of our UVES star WFI 507633 (topmost spectrum in the top panel) and star 206810 in NGC 6397 from the UVES archive (bottom spectrum in the top panel). The bottom panel shows the difference between the two spectra.

negligible within the quoted uncertainties. We note in passing that the major difference between the Gratton et al. (2001) and Korn et al. (2007) abundance determinations for these three stars lies in the v_t determination, which is approximately 0.5 km s^{-1} higher in the Korn et al. (2007) paper. This difference alone is probably enough to justify the different abundances found in the two studies.

Figure 7 compares the spectra of WFI 507633 and star 206810 in NGC 6397. The parameters of these stars are very similar, and indeed the calcium and iron lines are virtually identical, as confirmed by subtracting one spectrum from the other, where only noise remains. We are then confident that our analysis is correct and consistent with the one by Gratton et al. (2001), within the estimated uncertainties.

4. Abundance results

In the following sections we present and discuss abundance ratios of the measured elements. To compare with homogeneous literature sets, we considered preferentially large (≥10 stars) samples of high-resolution measurements of stars belonging to ω Cen. Unfortunately, there are no high-resolution studies of subgiants[13], so we resorted to red giants surveys (Norris & Da Costa, 1995; Smith et al., 2000; Johnson et al., 2009). This will help us to cross-identify sub-populations in the SGB region with those already identified on the RGB. For some species, there were no large literature surveys available, so we included articles based on smaller samples (<10 stars). The largest sample available to date is the one by Johnson & Pilachowski (2010), which contains more than 800 stars, but at a moderate resolution (R≃18 000). Their abundance ratio plots are more populous, but also obviously more scattered compared to higher-resolution studies, so we decided not to plot them in our Figures 8 to 13, except for their stars at [Fe/H]<–1.9 dex, which are not as well sampled in other less populous studies. We will also mention the abundace ratios by Villanova et al. (2010), a study of 38 stars observed in the external regions of ω Cen. Given the diversity of comparison studies, even if we reported all literature values to our solar abundance and loggf system (using lines in common) when possible, residual zeropoint differences among different studies will surely still be present.

[13] Although Villanova et al. (2007) study stars in the same evolutionary phase as our targets, their resolution is lower (R≃6000).

4.1. Iron

Our abundance ratios for iron and iron-peak elements are shown in Figure 8. We note that three of our six stars lie around [Fe/H]≃–2.0 dex, and that they do not correspond to any of the major sub-populations identified on the RGB, which are more metal-poor than any red giant studied with high-resolution spectroscopy before. The only exceptions are star ROA 213 by Smith et al. (2000), which has [Fe/H]=–1.97 dex, star 85007 by Villanova et al. (2010) at [Fe/H]=–1.98 dex, and a small group of 25 stars (out of more than 800) below [Fe/H]≃–2.0 dex in Figure 10 by Johnson & Pilachowski (2010). In their figure, the bulk populations have higher metallicities, with an abrupt drop in numbers below [Fe/H]≃–1.9 dex, approximately. We tentatively classify our three stars as a separate subgroup – containing few stars – that we name VMP (from very metal-poor, see also Section 5.1), and we will consider ROA 213 by Smith et al. (2000) and the 25 stars by Johnson & Pilachowski (2010) as the VMP counterparts on the RGB in the following discussion. The other three targets apparently fall into the metal-poor and metal-intermediate populations (MP and MInt, according to the classification by Pancino et al., 2000; Sollima et al., 2005a). We will discuss population identifications in more detail in Section 5.2.

We note that all comparisons in Figure 8 are between stars in different evolutionary phases (our targets are subgiants, while those in the literature are always giants). Therefore, the uncertainty on the zeropoint – especially as far as [Fe/H] is concerned – cannot be well quantified (see also Section 3.4). Possible factors that cause systematically discrepant abundances between giants and subgiants are

- there is still no consensus for the NLTE corrections to Fe I abundances, ranging from negligible (Gratton et al., 1999), to approximately 0.03–0.05 dex (Korn et al., 2007), to +0.3 dex (Thévenin & Idiart, 1999) for stars of the type presented here;
- the effect of diffusion could already be present for these subgiants, lowering abundance by an amount that could be negligible (Gratton et al., 2001) or of the order of 0.1–0.2 dex (Korn et al., 2007); however, diffusion is heavily influenced in all models by the amount of turbulent mixing, a phenomenon that is poorly constrained at present;
- there are also possible granulation inhomogeneities, which apparently go in the opposite direction compared to the above effects (Shchukina et al., 2005);
- finally, two studies that analysed these phenomena in NGC 6397 (Gratton et al., 2001; Korn et al., 2007) gave very different abundance results (see Section 3.5), so even from the observational point of view it is quite difficult to provide reliable constraints to these phenomena.

In spite of all these problems, we have the advantage that we do not use only [Fe/H], but we can also compare [El/Fe] abundance ratios – which should be more robust to measurement uncertainties and to variations caused by these physical processes – with a vast literature, to effectively cross-identify SGB and RGB populations.

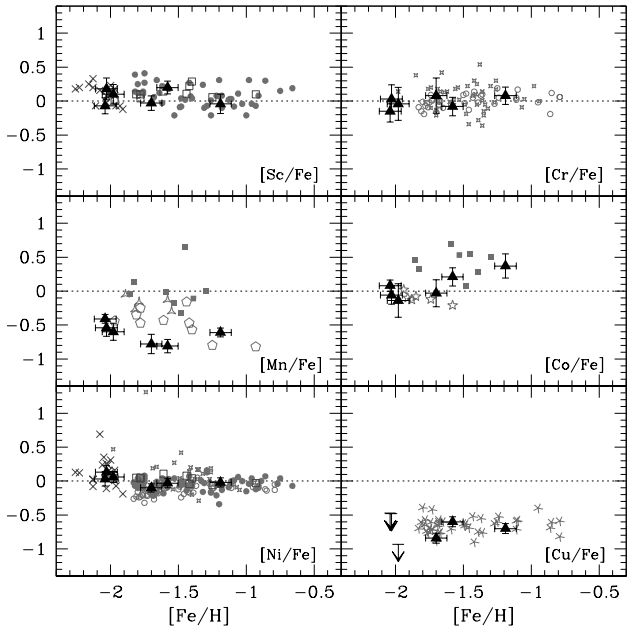

Fig. 8. Abundance ratios of iron-peak elements. Our measurements are marked with filled black triangles: error bars include random errors, continuum placement errors and errors owing to the choice of atmospheric parameters (see text). Grey symbols mark literature measurements for red giants: filled circles are from Johnson et al. (2009), empty pentagons from Cunha et al. (2010), empty circles from Norris & Da Costa (1995), empty triangles from Cohen (1981), filled squares from Gratton (1982), empty stars from François et al. (1988), asterisks from Cunha et al. (2002), crosses from Johnson & Pilachowski (2010), four-pointed stars from Villanova et al. (2010).

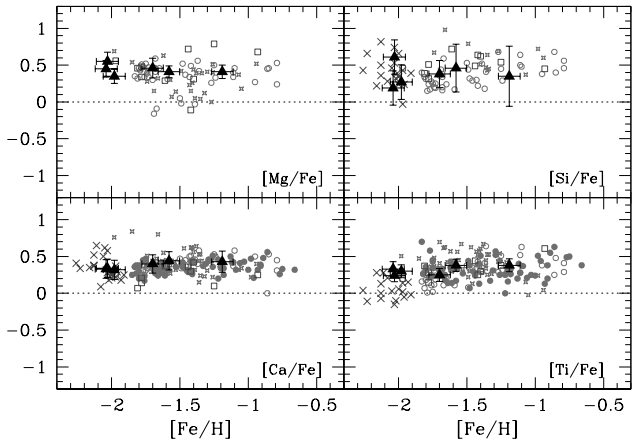

Fig. 9. Abundance ratios of α-elements. Symbols are the same as in Figure 8.

4.2. Iron-peak elements

While Norris & Da Costa (1995) provided Cr and Ni measurements for 40 red giants, Johnson et al. (2009) gave Ni measurements for 66 red giants and Cr for a smaller subset. Cr and Ni measurements are also provided by Villanova et al. (2010) for 30-35 stars. We took the Cunha et al. (2002) copper measurements for the 40 red giants already analysed by Norris & Da Costa (1995)[14]. For stars with [Fe/H]<–1.9 dex we used the Johnson & Pilachowski (2010) Sc and Ni measurements. No literature measurements in large samples of red giants were found for Co and Mn, except for the recent Mn study by Cunha et al. (2010), so we also compared with five giants by Cohen (1981), eight giants by Gratton (1982), and six giants by François et al. (1988).

There is general agreement for all iron-peak elements between our measurements for SGB stars and the literature RGB ones. Two odd elements, Sc and Co, would give better results if hyperfine splitting (HFS) was taken into account, but since they do not give any additional information with respect to Fe, traditionally no auhor has employed spectral synthesis to measure them. As a result, all ratios of Sc and Co in Figure 8 – including ours – are on average above solar. Our Sc values fall exactly on top of literature measurements, and our Co values for the three most metal-rich SGB stars lie between the Gratton (1982) and the François et al. (1988) measurements. It is known that large NLTE corrections are required for Co (Bergemann, 2010), which explains the rising trend observed in all cited studies. A slight underabundance can be noticed in the chromium ratios for the three most metal-poor stars, but NLTE effects should again be the cause for it (Bergemann, 2010). It is interesting to note that [Ni/Fe] tends to be slightly higher for the VMP stars than for the remaining three UVES targets by 0.1–0.2 dex, and that a similar trend can be noticed in Figure 10 by Johnson & Pilachowski (2010), who do not comment on this effect.

Mn and Cu are two very interesting elements with a dedicated vast literature because, although they belong to the iron-peak, they behave differently from other iron-peak elements (see McWilliam, 1997, for a classical review). In particular, Cu in ω Cen has been first measured by Pancino et al. (2002) on six RGB stars, and later studied in detail by Cunha et al. (2002), who found it underabundant similarly to field stars. Finally, it was theoretically modelled by Romano & Matteucci (2007), who found massive stars as the most likely producers of Cu, in agreement with previous studies (Bisterzo et al., 2004). While we find only upper limits for the three most metal-poor stars (Figure 8), our measurements agree with those by Cunha et al. (2002).

Manganese instead was found to be extremely underabundant in our six stars. The determinations by Cohen (1981) and Gratton (1982) appear only slightly subsolar, but none of these estimates takes into account HFS. A better agreement was found with the measurements by Cunha et al. (2010), based on the 10 stars by Smith et al. (2000), and derived with a complete HFS analysis, of which we plot the LTE resulting abundances in Figure 8. Our determinations, as those of Cunha et al. (2010), are lower than the values found for field stars (McWilliam, 1997) or metal-poor stars (Cayrel et al., 2004) around [Fe/H]=–2.0 dex. In particular, three of the five analysed lines belong to the 4000 Å resonance triplet which, according to Cayrel et al. (2004) gives systematically lower abundances by approximately 0.4 dex. Even rejecting these three lines, we found a [Mn/Fe]≃–0.7 dex for each of our six stars (Figure 8). The (marginal) discrepancy between our results and those by Cunha et al. (2010) could arise because we used the Mn lines around 4000 Å, while they use the lines around 6000 Å. The general result – that

[14] The Cu measurements of six stars by our group (Pancino et al., 2002) are in substantial agreement with the ones by Cunha et al. (2002), so we do not plot them in the various Figures.

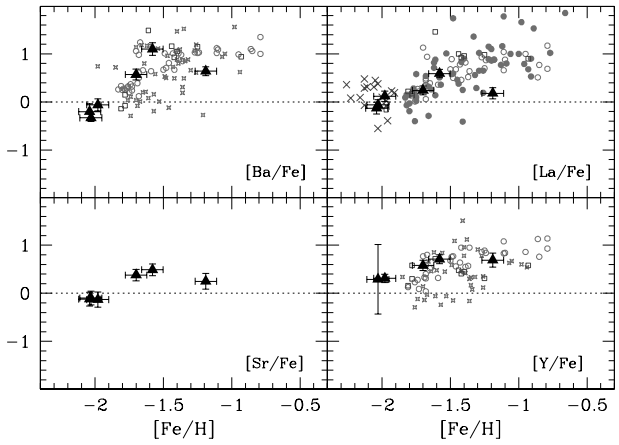

Fig. 10. Abundance ratios of heavy elements. Symbols are the same as in Figure 8.

ω Cen has lower Mn abundance than field and GGC stars – suggests that the source of Mn production in ωCen should be low-metallicity supernovae, either of type II or Ia (Cunha et al., 2010).

4.3. α-Elements

It was not possible to measure the oxygen lines, or to put meaningful upper limits to the oxygen abundance in these subgiants. We were able to measure Mg, Si, Ca and Ti (Figure 9): all four elements were present in the Norris & Da Costa (1995) and Smith et al. (2000) studies, but we plotted also the Ca and Ti more recent measurements by Johnson et al. (2009) and the Si, Ca, and Ti measurements for stars with [Fe/H]<–1.9 dex by Johnson & Pilachowski (2010). The measurements by Villanova et al. (2010) also include all four α-elements studies here.

All measurements are slightly dispersed for Si because only a handful of lines is generally available, while for the other three elements they show a reasonably small spread. The three VMP stars do not seem to show any difference from the other three SGB stars in their α-enhancement, with a weighted average of [α/Fe]=0.36±0.08 dex for all elements in all six stars. Literature measurements are quite scattered for Mg, but for RGB stars the Mg lines are very strong and difficult to measure, and Mg also anti-correrelates with Na, for example, so some spread should be expected. Apart from this exception, there is very good agreement among various literature determinations for giants, and with our measurements for subgiants. In particular, we note that RGB stars with [Fe/H]<–1.9 dex are always very close to our three VMP subgiants. The NLTE effects for all our SGB stars should be around ≃0.1 dex in size (Gratton et al., 1999), for Mg, but not all the lines analysed here were also analysed by Gratton et al. (1999), so we prefer not to apply any correction.

The α-enhancement of VMP, metal-poor, and intermediate stars in ω Cen is typical of the field stars of the Galactic halo, which is indicative of a chemical enrichment dominated by SNe II.

4.4. Heavy elements

We were able to measure Ba, La, Sr, and Y. For Ba and La we used spectral synthesis (see Sections 3.1 and 3.3) to take into account HFS. We plot the abundance ratios in Figure 10, along with the measurements by Norris & Da Costa (1995), Johnson et al. (2009), Villanova et al. (2010), and Johnson & Pilachowski (2010) for stars with [Fe/H]<–1.9 dex. The $\log gf$ used by Norris & Da Costa (1995) are now outdated, which is why, using the stars in common between literature studies (including Vanture et al., 1994; Smith et al., 2000; Pancino, 2003), we estimated that all their ratios needed to be raised by ≃0.4–0.5 dex – depending on the element – to compare with more recent studies. The Norris & Da Costa (1995) data appearing in Figure 10 are already corrected for this effect. Also, the solar Ba abundance by Villanova et al. (2010) was 2.31, while we use 2.13, and their data are corrected for this difference in Figure 10 as well.

The heavy s-process elements Ba and La generally agree with literature estimates. In particular, the VMP stars appear to have a lower average s-process enhancement, compatible with zero, as confirmed by the La measurements by Johnson & Pilachowski (2010). Thus, no s-process enrichment by AGB stars seems to have polluted the VMP star in the RGB, or in the SGB. This is supported by our Sr and Y measurements, which mainly agree with the literature measurements and which also have a low enhancement, compatible with zero for our VMP stars.

It is also interesting that the most metal-rich star in our sample, WFI 512115, appears to have a slightly lower s-process enhancement than other stars measured in the literature at similar metallicity. If confirmed by larger samples of metal-rich stars, this could point out that the s-process enrichment by AGB stars in ω Centauri was not completely homogeneous, as supported also by the small group of stars in the Norris & Da Costa (1995) sample, around [Fe/H]≃-1.7, which appears to have [Ba/Fe] 0.2–0.3 dex higher than other stars at similar metallicity. A larger spread was found by Villanova et al. (2010) in s-process elements than in other studies presented here, which they explain by assuming that a bimodality in these elements might be present at low metallicity, supporting the mentioned effect in the Norris & Da Costa (1995) data. Our three stars always share the same s-process enhancement, but larger samples are of course needed to see if the supposed bimodality, or higher spread, extends to -2.0 dex stars as well. Finally, there is a large fraction of stars with solar Ba and Y enhancement in the Villanova et al. (2010) sample at all metallicities, which are not present in any of the other studies of red giants in ω Cen, and it is not clear yet if this is because of an intrinsic feature of stars in the outskirts of the stellar system, or a spurious measurement effect.

4.5. Anti-correlations

Figure 11 shows the CH and CN band regions around 3880 and 4300 Å, respectively, for the three most metal-rich UVES stars. Clearly, two of them (namely WFI 503951 and 512115) show a deep CN band and almost no signal in the CH band. On the opposite, star WFI 503358 shows almost no CN band, and the CH band appears slightly deeper than in the other two stars. This evidence is not so clear in the three most metal-poor UVES stars, since the diatomic CN molecular band is much shallower.

We also have atomic lines of other elements that are found to (anti-)correlate within Galactic globular clusters, namely Mg, Na, and Al, besides C and N. Their abundance ratios are

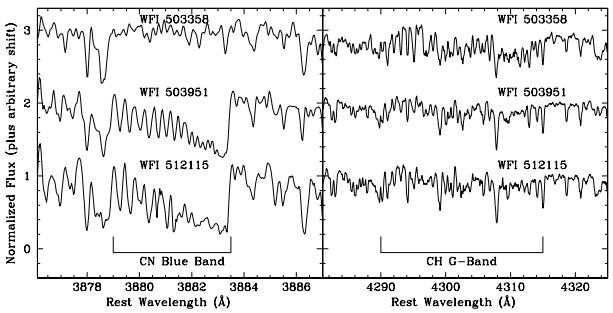

Fig. 11. Smoothed spectra of the three most metal-rich UVES targets around the CN and the CH blue bands.

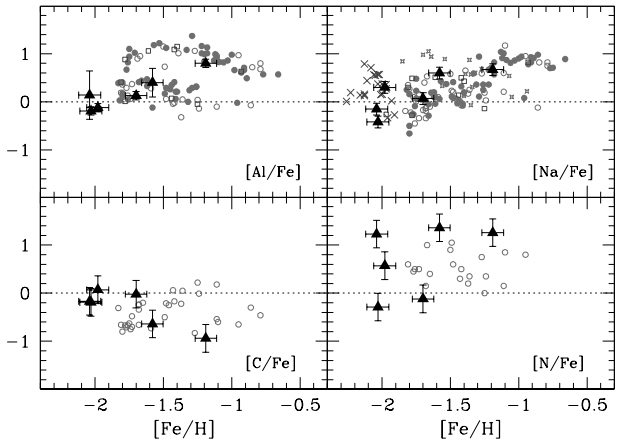

Fig. 12. Abundance ratios of Al, Na, C, and N for the six UVES stars. Symbols are the same as in Figure 8.

plotted in Figures 9 and 12. An initial observation is, looking at the literature abundance ratio plots (Norris & Da Costa, 1995; Johnson et al., 2009; Johnson & Pilachowski, 2010; Marino et al., 2010) that [Al/Fe] and [Na/Fe] appear clearly bimodal at all metallicities (with the possible exception of the most metal-rich stars around [Fe/H]≃–0.6 dex), with two distinct sequences around [Al/Fe]≃0 and [Al/Fe]≃1 dex in the case of aluminium, and the same bimodality is visible, although less clearly, in the C and N ratios. In our Figure 12 the Na data are confused because the Villanova et al. (2010) data have an opposite trend to all the other literature data plotted, with Na decreasing with metallicity instead of increasing with it. We found no explanation for this trend. Apart from this, our data follow the literature trends reasonably well, with a similarly large scatter for [N/Fe]. We did not apply NLTE corrections following a reasoning similar to that of Mg in Section 4.3, but they should be again around 0.1 dex for these subgiants (Gratton et al., 2001).

Figure 13 reports on the usual (anti-)correlation plots. A clear and bimodal Na-Al correlation is seen in the literature data, as well as the C-N anti-correlation. Our data compare well with the literature in both cases. Even the most difficult Mg-Al anti-correlation is clearly visible in the literature data, although not as clearly in our own data for the six UVES stars. Finally, we also report the C-Al anti-correlation in Figure 13.

In summary, two of the three most metal-rich stars show clear signs of CNO pollution, as well as a clear Na-Al

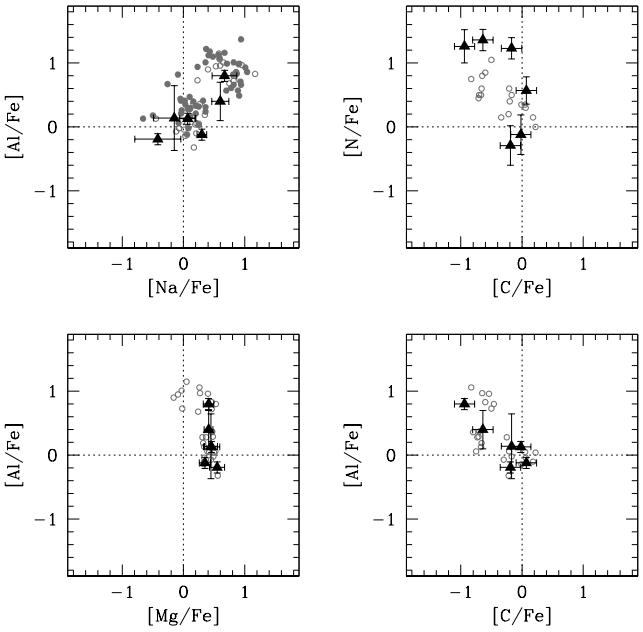

Fig. 13. Anti-correlation plots for the six UVES stars. Symbols are the same as in Figure 8.

anti-correlation, and this agrees with all past literature data on the subject. Our data for the three VMP stars are instead not conclusive about the presence of (anti-)correlations in the VMP population as a whole. We have two stars (WFI 507109 and 512938) with primordial composition and one star (WFI 507633) that seems to have high [N/Fe], but solar [C/Fe]. Literature measurements seem to point towards absent or reduced (anti-)correlations in VMP stars. The 25 stars by Johnson & Pilachowski (2010) with [Fe/H]<–1.9 dex tend to all have high sodium, and a much lower dispersion than the other >800 stars in their sample. But there are no Al, Mg, C, or N measurements in their study. On the other hand, Marino et al. (2010) show that for their red giants with [Fe/H]<–1.8 dex, the Na-O anti-correlation appear less extended than that for other metallicity groups in ω Cen, but we do not know how the situation stands for [Fe/H]<–1.9 dex only.

While a complete discussion on the anti-correlations among light elements in ω Centauri is beyond the scope of the present paper – for the moment we just want to cross-identify our SGB stars with the RGB populations – we confirm that whatever the cause of anti-correlations in GC, it must have been active on each sub-population of ω Cen, possibly excluding only the most metal-poor one, at [Fe/H]≃–2.0 dex, and the most metal-rich one (where all stars above –1.0 dex appear polluted, Marino et al., 2010). The presence or absence of (anti-)correlations in some sub-populations of ω Cen is a powerful tool to understand its chemical evolution (see Pancino, 2003; Carretta et al., 2010, and the discussion in Section 5.1).

5. Discussion

While comparisons between subgiants and giants are not entirely free from problems (see e.g., Bonifacio et al., 2009, and references therein), we measured abundance ratios of several species, in good agreement with past literature determination for RGB stars. We found that three of our targets seem to belong to a sepa-

rate population with typical [Fe/H]≃–2.0 dex, [α/Fe]≃+0.35 dex, and an *s*-process enhancement compatible with zero. Of the three remaining stars, two are consistent with the abundance ratios of the RGB-MP (nomenclature by Pancino et al., 2000), and the last star appears to belong to the RGB-MInt population (nomenclature by Pancino et al., 2000) or, more specifically, to the RGB-MInt2 (nomenclature by Sollima et al., 2005a).

With this identification as our compass, we will try in the following sections to contribute to the understanding of the SGB of ω Cen on a few crucial topics.

5.1. The first stellar generation in ω Cen?

As discussed in Section 4.1, the three most metal-poor stars at [Fe/H]≃–2.0 dex appear to belong to a separate sub-population, which we termed VMP (for very metal-poor). Stars as metal-poor as these were found in the past in small amounts, but were not considered as a separate sub-population per se. In particular, several (unbiassed with respect to metallicity) studies, aimed at deriving the metallicity distribution of ω Cen either through photometry (Frinchaboy et al., 2002; Sollima et al., 2005a; Calamida et al., 2009), low-resolution spectroscopy of red giants (Norris et al., 1996; Suntzeff & Kraft, 1996), or subgiants (Sollima et al., 2005b; Stanford et al., 2006; Villanova et al., 2007) found stars as poor as –2.0 dex or lower. Some high-resolution abundance studies also found again a few VMP stars (Smith et al., 2000; Johnson et al., 2009; Johnson & Pilachowski, 2010; Marino et al., 2010; Villanova et al., 2010), and in general there appears to be an abrupt termination of the main MP population around [Fe/H]≃–1.9 dex, with a sparse group of stars around [Fe/H]≃–2.0 dex. This effect is clearly visible in Figure 10 by Johnson & Pilachowski (2010). This clean behaviour justifies the definition of VMP as a new, separate sub-population in ω Cen.

To estimate the fraction of such a minority population is not easy. From the cited studies we estimate that it should be at most 5% of the entire stellar content of ω Cen. Some more support to the existence of this small VMP component comes from the recent work by Bellini et al. (2010), who used exquisite ACS photometry to reveal additional sub-structure in the SGB region of ω Cen. In particular, the upper SGB branch (branch A in the nomenclature of Villanova et al., 2007) appears split into two sub-branches in Bellini et al. (2010). The fact that three out of three of our upper SGB targets turned out to have [Fe/H]=–2.0 dex can thus be explained, because we chose them on the upper evelope of the upper branch, which turns out to be separated from the other branches, and which we can safely consider to be made of [Fe/H]=–2.0 dex stars, at least in the external region of ω Cen that we are sampling here (see Figure 2).

Our abundance ratios, based on high-resolution spectroscopy, allow us to hypothesize that these stars must be the best candidate remnant of the primordial population in ω Centauri, enriched primarily by type II SNe (given its [α/Fe]≃+0.35 dex), and most probably free from severe pollution by AGB stars. This last statement is supported by the (almost) solar *s*-process ratios (Figure 10). Also, while three stars are too few to rule out the presence of anti-correlations in this population, literature studies (Smith et al., 2000; Johnson et al., 2009; Johnson & Pilachowski, 2010; Marino et al., 2010) suggest that (anti-)correlations should be absent or reduced in their extension for VMP stars. It would be *extremely* interesting to study C, N, Mg, Na, and Al in larger samples of SGB stars in ω Cen. Indeed, although ω Cen is commonly considered as the remnant of a dwarf galaxy accreted a long time ago by the Milky Way, all the sub-populations identified so far show clear anti-correlations (Figures 12 and 13) at all metallicities, except for – possibly – the VMP and RGB-a stars (Marino et al., 2010). Field populations of dwarf galaxies do not normally show any anti-correlation, which is only found in globular clusters (Gratton et al., 2004). Therefore, the absence (or existence) of anti-correlations in the VMP component could give us evidence for (or against) the dwarf galaxy hypothesis for the origin of ω Centauri, as discussed also by Pancino (2003) and (Carretta et al., 2010).

Summarizing, given the chemical properties of the VMP stars studies here and in the cited high-resolution studies, we conclude that they belong to a small and distinct sub-population, which appears to be the best-candidate (remnant) population of the first stellar generation in ω Cen, but could also – if the presence of (anti)-correlations will be excluded – be the field population remnant of its hypothesized parent galaxy.

5.2. SGB populations puzzle: who is who

Apart from the notation used above, which separates the ω Cen sub-populations by metallicity in VMP, MP, MInt (in turn divided in Int1, Int2, and Int3), and MR (or RGB-a and SGB-a) proposed by Pancino et al. (2000), Ferraro et al. (2004) and Sollima et al. (2005a), we will also use the nomenclature by Villanova et al. (2007) in this Section, who photometrically divide the SGB into four sub-branches (A, B, C and D) from the upper SGB envelope down to the SGB-a. This classification is also put into evidence in the two leftmost panels of Figure 14.

The whole difficulty in the study of the SGB of ω Cen is to cross-correlate the five sub-populations defined photometrically and spectroscopically along the RGB with the four or five (and more, see Bellini et al., 2010) sub-branches that are visible on the SGB. This is because, while on the RGB there are exquisite high-resolution studies that can link photometric features with chemical abundance patterns, this is not yet possible for the SGB. One important observation suggested by past attempts to link SGB and RGB populations is that the nicely combed structure that appears in the RGB and the similarly nicely combed one that appears on the SGB could be somehow scrambled and mixed, as pointed out by Villanova et al. (2007). While on the RGB the dominating factor that separates populations is metallicity, on the SGB it must be age (together with C, N, O, and He), and this could complicate things significantly if there were no clear (monotonic increasing) age-metallicity relation in ω Cen. The uncertainties involved in the past low-resolution spectroscopic studies such as Sollima et al. (2005b) and Villanova et al. (2007) were apparently not sufficient to give a final answer to the problem. The present study, on the other hand, while having higher precision in the abundance determination, can only rely on a limited number of stars.

5.2.1. The VMP population

Concerning our newly defined VMP population, we must assume that it should lie: *(i)* on the bluest egde of the RGB colour distribution, because of its low metallicity, and *(ii)* on the upper edge of the SGB, and in particular on the upper edge of branch A by Villanova et al. (2007), where we find three stars out of three at [Fe/H]≃–2 dex. This is supported by Figure 12 by Bellini et al. (2010), where for the first time the upper SGB appears split into two separate branches, and where the lower base of the RGB shows a clearly bluer sub-sequence made of a small

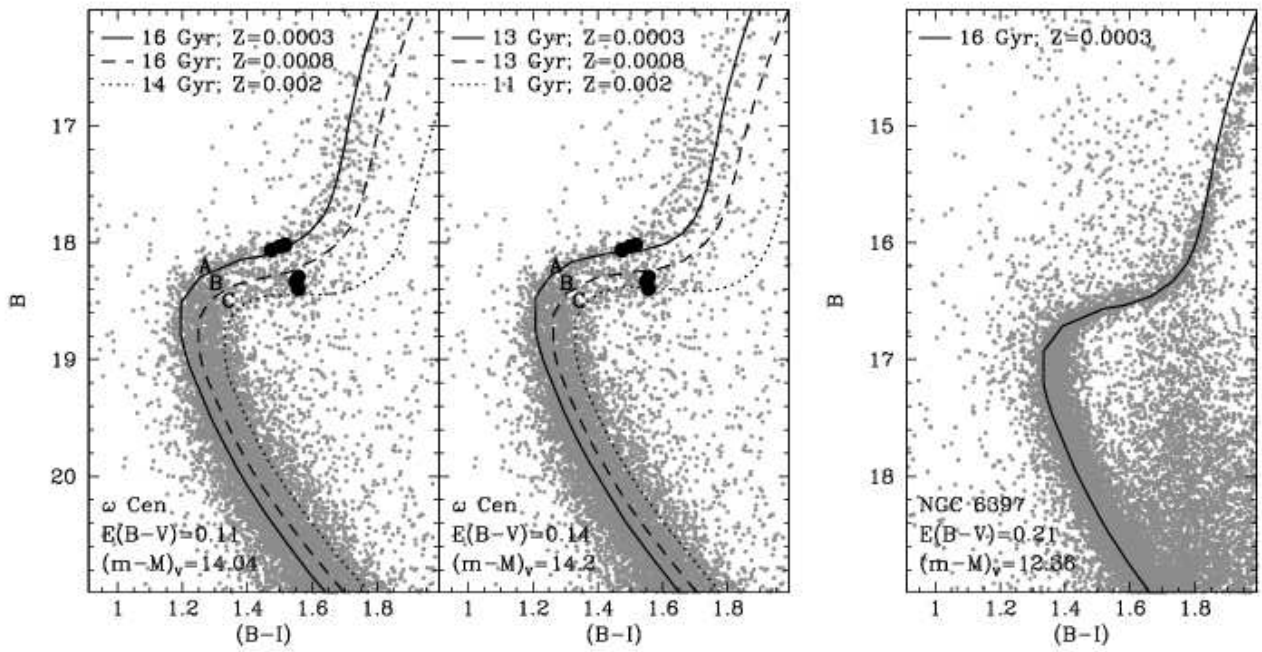

Fig. 14. An example of isochrones fit (see text) to determine age differences among the three sub-populations studied in this paper. Left panel: the literature values of E(B–V) and (m-M)$_V$ for ω Cen are used to derive age differences; the oldest populations turns out to be 16 Gr old. Centre panel: a cosmological age of 13 Gyr is forced for the oldest populations, altering E(B–V) and (m-M)$_V$ but with no significant effect on the resulting age differences; the shape of the isochrones is now in worse agreement with the data. Right panel: NGC 6397 is shown for comparison. The letters A, B, and C, which appear in the two leftmost panels, indicate the approximate location of the SGB branches as defined by Villanova et al. (2007).

number of stars. These features are the most likely photometric counterparts of the VMP population found here.

5.2.2. The MP population

The connection between the SGB-MP and the RGB-MP is not clear yet. While *some other population* should be present together with the VMP to account for the number of stars in the upper branch, or branch A, it is not clear if this is really the counterpart of the RGB-MP, because the RGB-MP contains at least 30% (and likely more) of the stars in ω Cen. We cannot speculate too much with the data in hand – the only certain fact is that the two MP stars in this paper (WFI 503358 and 503951) both lie lower than branch A, possibly on branch B or even C – but we see two possible solutions:

- One possibility – supported by our analysis of stars WFI 503358 and 503351 – is that the RGB-MInt1 stays on branch A (lower half) together with the VMP, and the RGB-MP stays instead on branch B. This would allow for a better agreement between the population fractions estimated by Sollima et al. (2005a) and Villanova et al. (2007), while the uncertainties of both low resolution studies are probably large enough to accommodate such a switch.
- The other obvious interpretation has been already mentioned by Villanova et al. (2007), i.e., that MP stars lie on both branches A (lower) and B, mixed with part of the metal-intermediate populations.

5.2.3. The MInt populations

Our star WFI 512115, which chemically belongs to the MInt population (and, more specifically, to the MInt2) also appears to lie either on branch B or – most probably – on branch C. Combining this evidence with the one presented by both Sollima et al. (2005b) and Villanova et al. (2007), we tentatively conclude that the most likely photometric counterpart of the MInt2 population should be branch C. The presence of a few RGB-MP stars on branch C still cannot be ruled out, and it could be either caused by some scatter in the low-resolution abundances by Villanova et al. (2007), or by photometric errors in the WFI reference photometry (Pancino et al., 2000; Pancino, 2003), or even by a different SGB shape for the SGB-MP (Bellini et al., 2010). We also speculate that the RGB-MInt3 should correspond to a sequence lying between branches C and D, as clearly indicated by Sollima et al. (2005b) in their Figure 4, and mentioned in passing by Villanova et al. (2007).

5.2.4. The MR or SGB-a population

While the cross-identification between the RGB-a (Pancino et al., 2000; Sollima et al., 2005a), the SGB-a Ferraro et al. (2004); Sollima et al. (2005b) and branch D (Villanova et al., 2007) appears unquestionable, there is still some debate about its metallicity, ranging from [Fe/H]$\simeq$–1.1, derived from low-resolution spectroscopy of SGB stars by Villanova et al. (2007) to [Fe/H]$\simeq$–0.6 dex, derived from both high-resolution spectroscopy of RGB stars (Pancino et al., 2000) and low-resolution spectroscopy of SGB stars (Sollima et al., 2005b). The metallicity of the SGB-a will be the subject of a following paper based on GIRAFFE data, but it is interesting to

note here that Bellini et al. (2010) found the SGB-a (or branch D) split into two sequences, suggesting that two populations with slightly different properties could occupy these two very close loci.

5.3. Towards a solution of the age spread problem

The history of age spread determinations in ω Cen comprises a variety of studies, all focused on the SGB, the most age sensitive region in the CMD. An age spread of 2–5 Gyr, among the various sub-populations was first found by Hughes & Wallerstein (2000) and Hilker & Richtler (2000), based on the TO region morphology of their high-quality Strömgren photometries and colour-metallicty calibrations. Later several other papers came out based on combinations of high quality photometry and low-resolution spectroscopy (Hughes et al., 2004; Hilker et al., 2004; Rey et al., 2004; Sollima et al., 2005b; Stanford et al., 2006; Villanova et al., 2007), finding again various age dispersions all around 2–5 Gyr. The only studies reporting on age difference below 2 Gyrs are those by Ferraro et al. (2004), who find that the SGB-a cannot be fitted with any isochrone younger than the SGB-MP population, and Sollima et al. (2005b), who similarly found that the overall age spread of the SGB sub-populations cannot amount to more than 2 Gyr. It is interesting to note that Sollima et al. (2005b) and Villanova et al. (2007) use photometry from the same ACS data set and spectra of similar quality, and reach opposite conclusions, with Villanova et al. (2007) finding an age spread of at least 2 Gyr within the MP population only.

On the one hand, spectroscopic abundances of both RGB and SGB stars find an α-enhancement of all populations (except the RGB-a) consistent with pure type II SNe enrichment which, in the self-enrichment scenario for ω Cen, would imply very fast enrichmemt, within 1 Gyr. On the other hand, the high *s*-process enhancement of all populations (except maybe the VMP found here) would imply enrichment by intermediate mass (1–3 $M_{\odot}$) AGB stars on longer timescales (1–2 Gyr and possibly even more Busso et al., 1999). Therefore, if ω Cen is a self-enriched system, we should find (and indeed many authors do find) some significant age spread. While we cannot give the ultimate solution to the relative ages (or age spread) puzzles listed above with the present data, we can nevertheless use our newly defined VMP population to shed some light on the problem.

We use isochrones from the Padova database of stellar evolutionary tracks and isochrones[15], and in particular we chose the ones based on the Marigo et al. (2008) and Girardi et al. (2000) tracks. We preferred this set over BaSTI[16] (Pietrinferni et al., 2006) simply because they provide tranformations to the WFI filters. We note that the results in ages do not change significantly when using BaSTI (less than 1≃Gyr overall shift), but the actual shape of the SGB is better reproduced when the WFI filters are used instead. While the absolute ages are somewhat uncertain, we show in Figure 14 that the age differences are relatively robust regardless of the absolute age scale calibration of the chosen isochones set.

Firstly, we computed the Z values for the three populations using the formula

$$\log Z = [\mathrm{Fe/H}] - 1.7 + \log(0.638\ 10^{\ [\alpha/\mathrm{Fe}]} + 0.362)$$

according to Salaris et al. (1993). We adopted the Lub (2002) reddening and Bellazzini et al. (2004) distance modulus (see also Section 3.2). We used the cosmological helium abundance models (for a discussion on higher He abundances see Section 5.4). The uncertainties involved in the isochrone fitting procedures are large: we assume aproximately ±2 Gyr. We find that the VMP and MP populations must be relatively close in age, with a difference of 0±2 Gyr, while the MInt component should be about 2±2 Gyr younger. If we force the age of the oldest population(s) to a cosmological value of 13 Gyr, we have to increase E(B–V) and $(m–M)_V$ by 0.03 and 0.16 mag respectively, and the fit becomes considerably worse when considering the isochrones shape. The age differences, however, do not change. As a comparison, we show in Figure 14 the case of NGC 6397, using the WFI B, V, and I photometric catalogue described by Carretta et al. (2009) and the reddening and distance modulus from the revised Harris (1996) catalogue.

The existence of the VMP at the SGB level could help in solving two of the paradoxes previously found in the literature. The first is the zero age difference – within the uncertainties – found by Sollima et al. (2005b) between the MP and the MInt populations, which is difficult to understand given the difference in s-process enhancement between the two populations. If one assigns [Fe/H]=–2 dex to the upper SGB envelope, and moves the MP population to branch B, this shift in metallicity would be allowed by the uncertainties in the Sollima et al. (2005b) low-resolution spectroscopy (see also Starkenburg et al., 2010, on the uncertainties of the calcium triplet calibration at low metallicity). As a result, the MP would become older, and the age difference between the MP and MInt populations would not be so close to zero anymore.

The second puzzle that could be alleviated by the existence of the VMP is the coexistence within the MP group of two separate populations with ages differing by ≃2–3 Gyr, found by Villanova et al. (2007), which could be explained if one admits that the MP population is in reality a mix of MP and VMP stars. The metallicity difference between the VMP and MP populations would be difficult to resolve with low-resolution spectroscopy, similarly to the case above. The younger MP group identified by Villanova et al. (2007) would become older if its metallicity was [Fe/H]≃–2.0 dex instead of –1.7 dex, thus recreating an almost monotonic age-metallicity relation, although the age difference between the VMP and the MP populations would be small. It could be argued that the younger MP in Villanova et al. (2007) is much more numerous than the VMP estimated fraction, i.e., 5% of the total stellar content in ω Cen. However, we must note that a large fraction of the targets in that study are selected *a priori* on the upper SGB branch (or branch A), which we suspect is dominated by VMP stars. In this case, the target selection would be biassed preferentially towards the VMP population and the relative numbers in Figure 19 by Villanova et al. (2007) would not be representative of the respective population fractions anymore.

In a self-enrichment scenario, the small age difference between the VMP and the MP population (0±2 Gyr) poses no problem as far as the type II SNe are concerned, but could perhaps be too short to accommodate the ≃0.5 dex overabundance in s-process elements for the MP. On the other hand, if 2±2 Gyr occurred between the MP and the MInt2 population, there could be enough time to enrich the MInt population in s-process elements up to the observed level of [s/Fe]≃1 dex. Detailed chemical evolution calculations would be extremely useful in understanding these details.

[15] http://pleiadi.pd.astro.it/

[16] www.oa-teramo.inaf.it/BASTI/

5.4. The helium abundance

Since the discovery of a double MS in ω Cen (Anderson, 2002; Bedin et al., 2004), and the evidence that the bluer sequence was more metal-rich than the redder one (Piotto et al., 2005), it was suggested that some of the metal-richer populations in ω Cen could have abnormal He abundance (Norris, 2004), of about Y≃0.35–0.40. A recent review by Renzini (2008) discussed the possible scenarios and compared them with observations of ω Cen, but also of NGC 2808, which was found to possess a triple MS (Piotto et al., 2007), along with other massive GGC.

Such an overabundant helium would have some impact in the model atmospheres (Böhm-Vitense, 1979; Girardi et al., 2007) that are at the basis of any abundance analysis such as the one presented here. The first thing to note is that the most metal-poor populations of ω Cen do not require any He enhancement, and we assume this to be the case not only for the two MP stars (WFI 503358 and 503951), but also for the three VMP ones (WFI 507109, 507633, and 512938). The only star that could suffer from an helium enriched atmoshpere is the one belonging to the MInt2 population, WFI 512115.

A simplified treatment by Gray (2008) assumes that an overabundance in helium has a similar effect as an increase in gravity, as a first approximation:

$$\frac{\Delta g}{g} = \frac{4\,\Delta A(\mathrm{He})}{1 + 4\,A(\mathrm{He})}.$$

Just to derive an order-of-magnitude effect, we translate a mass fraction increase from Y≃0.25 to Y≃0.35 into a number increase from A(He)≃0.10 to A(He)≃0.15. This would be mimicked, in our WFI 512115 star, by an increase in surface gravity from roughly 3.5 to 4.0 dex, corresponding to an increase in abundance of 0.08 dex in [Fe/H]. Thus, WFI 512115 would change from [Fe/H]=–1.19 to –1.11 dex, with basically no significant effect in the age difference determination, within the quoted uncertainties. We finally note here that, as discussed by Sollima et al. (2005b) in their Figure 6, this increase in the helium abundance would only change the *shape* of the isochrone's SGB, making it steeper, with a negligible (less than 1 Gyr) impact on the relative age determination.

6. Summary and Conclusions

We analysed UVES high-resolution spectra of six stars on the SGB of ω Centauri. We compared our results with RGB high-resolution spectroscopy to identify the sub-populations to which our targets belong, and we found remarkable agreement with past abundance determinations. Three of our targets (WFI 507109, 507633, and 512939) have [Fe/H]≃–2.0 dex, are α-enhanced and show no significant s-process enhancement. Two of the remaining targets (WFI 503358 and 503951) belong to the MP population, with [Fe/H]≃–1.65 dex, α-enhanced and with [s/Fe]≃+0.5 dex. The last target, star WFI 512115, belongs to the MInt2 population, with [Fe/H]=–1.19 dex, α-ehanced and with s-process enhancement similar to the MP targets, i.e., slightly lower than what is expected for MInt stars.

Our main result (see Section 5.1) is that *there exists an additional, metal-poor population (that we name VMP) at [Fe/H]≃–2.0 dex, which has chemical properties that make it the ideal candidate (remnant of) the primordial population of ω Cen.* The RGB star ROA 213 Smith et al. (2000), star 85007 by Villanova et al. (2010), and 25 red giants studied by Johnson & Pilachowski (2010), have similar chemical composition and could represent the prototype VMP members along the RGB. In particular, the s-process enhancement of the SGB-VMP population is not compatible with the RGB-MP stars, while it is compatible with the quoted RGB-VMP stars. Our conclusion is also supported by previous work on metallicity distributions or RGB and SGB stars and by the exquisite photometry by Bellini et al. (2010). We estimate that this VMP population should comprise at most 5% of the entire stellar content of ω Centauri, at present. The presence or absence of light element anti-correlations in this population would be a fundamental constraint to the nature of ω Cen, because anti-correlations are generally exclusively found in globular clusters and never in the field populations of galaxies. From the available literature (mainly Johnson et al., 2009; Johnson & Pilachowski, 2010; Marino et al., 2010) it appears that (anti-)correlations could be reduced in extent, in VMP stars. Until the presence of (anti)-correlations in VMP stars is excluded by larger data samples, it looks more promising to interpret this as the primordial population of ω Cen instead of the remnant field population of its putative parent galaxy.

The high-precision abundance determinations obtained allowed us to try to shed some light on the SGB morphology relation with the RGB spectroscopically identified sub-populations. We conclude that *there appears to be no one-to-one correspondence between the nicely combed substructures of the RGB and SGB. In particular, the MP and MInt populations could either be mixed along the (lower) A, B, and C branches, or be positioned in a not strictly monotonic order, with MInt1 occupying branch A (lower) and MP branch B, just as an example.* As already said, VMP stars should occupy (and possibly dominate) the uppermost SGB branch, or branch A in the Villanova et al. (2007) terminology.

We also found that (see Section 5.3) *the existence of the VMP population could alleviate some of the problems found in previous determinations of relative ages.* In particular, the small metallicity difference between the VMP and MP populations could have escaped previous abundance analyses based on low-resolution spectra. The puzzling result by Villanova et al. (2007) that the MP population should contain two groups with different ages could indeed be explained by the metallicity difference between VMP and MP. Also, the (too) small age difference found by Sollima et al. (2005b) between the MP and MInt populations woul become slightly larger when taking into account the existence of the VMP, which should dominate the uppermost SGB envelope.

Finally, *there should be a small age difference between the VMP and MP populations (0±2 Gyr), while a slightly larger age difference (2±2 Gyr) should occur between the VMP and the MInt2 populations.* Althought this latter result is less secure because it relies on one star only, it agrees very well with the majority of past studies (see, e.g., Stanford et al., 2006). The use of different sets of isochrones (Padova, BaSTI) does not change the result significantly, and the helium abundance problem should have a negligible impact on the MInt2 star WFI 512115 (the only one which should have higher helium) because, to first approximation, it should change its [Fe/H] by ≃0.08 dex. The age distribution suggested by the present data would accommodate a fast enrichment between the VMP and MP populations, dominated by SNe type II, while the s-process enrichment of the MP ([s/Fe]≃+0.5 dex) could still pose a problem. The age difference between the MP and MInt populations could instead be sufficient to allow for some intermediate-mass AGB star enrichment (Busso et al., 1999), bringing [s/Fe] to +1.0 dex.

We conclude by noting that this is the only high-resolution-based abundance analysis published on SGB stars in ω Cen so far. Even if the precision of the abundances is higher than in past low-resolution studies, of course the number of stars examined is only six. To give the final answer to the relative ages problem in ω Cen, and to identify who is who in the CMD at the SGB level, a much larger sample (a few hundreds) of relatively high-resolution spectra in the SGB region is absolutely necessary.

Acknowledgements. We would like to thank A. Sollima for help with isochrone fits, P. Bonifacio, and S. Villanova for detailed comments on the abundance analysis and age spread discussion. EP acknowledges the ESO *Visitor Programme* in Chile, where part of this work was done.

References

Ali, A. W., & Griem, H. R. 1965, Physical Review , 140, 1044
Alonso, A., Arribas, S., & Martínez-Roger, C. 1999, A&AS, 140, 261
Andersen, J., 1999, Transactions of the IAU Vol. XXIII B, Dordrecht: Kluwer
Anderson, J. 2002, Omega Centauri, A Unique Window into Astrophysics, 265, 87
Ballester, P., Modigliani, A., Boitquin, O., Cristiani, S., Hanuschik, R., Kaufer, A., Wolf, S., 2000, The ESO Messenger, 101, 31
Bedin, L. R., Piotto, G., Anderson, J., Cassisi, S., King, I. R., Momany, Y., & Carraro, G. 2004, ApJ, 605, L125
Bellazzini, M., Ferraro, F. R., Sollima, A., Pancino, E., & Origlia, L. 2004, A&A, 424, 199
Bellini, A., et al. 2009, A&A, 493, 959
Bellini, A., Bedin, L. R., Piotto, G., Milone, A. P., Marino, A. F., & Villanova, S. 2010, AJ, 140, 631
Bergbusch, P.A., VandenBerg, D.A., 2001, ApJ, 556, 322
Bergemann, M. 2010, arXiv:1009.5693
Bessell, M. S. 1979, PASP, 91, 589
Bielski, A. 1975, JQSRT 15, 463
Bisterzo, S., Gallino, R., Pignatari, M., Pompeia, L., Cunha, K., & Smith, V. 2004, Mem. Soc. Astron. Italiana, 75, 741
Böhm-Vitense, E. 1979, ApJ, 234, 521
Bonifacio, P., Molaro, P., Beers, T. C., & Vladilo, G. 1998, A&A, 332, 672
Bonifacio, P., et al. 2009, A&A, 501, 519
Busso, M., Gallino, R., & Wasserburg, G. J. 1999, ARA&A, 37, 239
Calamida, A., et al. 2009, ApJ, 706, 1277
Carretta, E., et al. 2009, A&A, 505, 117
Carretta, E., et al. 2010, ApJ, 714, L7
Cayrel, R. 1988, The Impact of Very High S/N Spectroscopy on Stellar Physics, 132, 345
Cayrel, R., et al. 2004, A&A, 416, 1117
Cohen, J. G. 1981, ApJ, 247, 869
Cunha, K., Smith, V. V., Suntzeff, N. B., Norris, J. E., Da Costa, G. S., & Plez, B. 2002, AJ, 124, 379
Cunha, K., Smith, V. V., Bergemann, M., Suntzeff, N. B., & Lambert, D. L. 2010, arXiv:1005.2363
Dean, J. F., Warren, P. R., & Cousins, A. W. J. 1978, MNRAS, 183, 569
Ferraro, F. R., Sollima, A., Pancino, E., Bellazzini, M., Straniero, O., Origlia, L., & Cool, A. M. 2004, ApJ, 603, L81
Francois, P., Spite, M., & Spite, F. 1988, A&A, 191, 267
Frinchaboy, P. M., et al. 2002, Omega Centauri, A Unique Window into Astrophysics, 265, 143
Girardi, L., Bressan, A., Bertelli, G., & Chiosi, C. 2000, A&AS, 141, 371
Girardi, L., Castelli, F., Bertelli, G., & Nasi, E. 2007, A&A, 468, 657
Gratton, R. G. 1982, A&A, 115, 336
Gratton, R. G., Carretta, E., Eriksson, K., & Gustafsson, B. 1999, A&A, 350, 955
Gratton, R. G., et al. 2001, A&A, 369, 87
Gratton, R., Sneden, C., & Carretta, E. 2004, ARA&A, 42, 385
Grevesse, N., Noels, A., & Sauval, A. J. 1996, Cosmic Abundances, 99, 117 Observatory
Gray, D. F. 2008, The Observation and Analysis of Stellar Photospheres, by D.F. Gray. Cambridge: Cambridge University Press, 2008
Harris W.E., 1996, AJ, 112, 1487
Hilker, M., & Richtler, T. 2000, A&A, 362, 895
Hilker, M., Kayser, A., Richtler, T., & Willemsen, P. 2004, A&A, 422, L9
Hoffleit D., Jaschek C., 1991, The Bright Star Catalogue, 5th revised edition, New Haven: Yale University
Hughes, J., & Wallerstein, G. 2000, AJ, 119, 1225
Hughes, J., Wallerstein, G., van Leeuwen, F., & Hilker, M. 2004, AJ, 127, 980
Johnson, C. I., Pilachowski, C. A., Simmerer, J., & Schwenk, D. 2008, ApJ, 681, 1505
Johnson, C. I., Pilachowski, C. A., Michael Rich, R., & Fulbright, J. P. 2009, ApJ, 698, 2048
Johnson, C. I., & Pilachowski, C. A. 2010, ApJ, 722, 1373
Korn, A. J., Grundahl, F., Richard, O., Mashonkina, L., Barklem, P. S., Collet, R., Gustafsson, B., & Piskunov, N. 2007, ApJ, 671, 402
Kupka, F., Piskunov, N., Ryabchikova, T. A., Stempels, H. C., & Weiss, W. W. 1999, A&AS, 138, 119
Kurucz, R. L., & Peytremann, E. 1975, SAO Special Report, 362,
Kurucz, R. 1993, SYNTHE Spectrum Synthesis Programs and Line Data. Kurucz CD-ROM No. 18. Cambridge, Mass.: Smithsonian Astrophysical Observatory, 1993., 18
Kurucz, R. L. 2005, Memorie della Società Astronomica Italiana Supplementi, 8, 14
Lawler, J. E., Bonvallet, G., & Sneden, C. 2001, ApJ, 556, 452
Lee, Y.-W., Joo, J.-M., Sohn, Y.-J., Rey, S.-C., Lee, H.-C., & Walker, A. R. 1999, Nature, 402, 55
Lub J., 2002, ASP Conf. Ser. 265: Omega Centauri, A Unique Window into Astrophysics, 95
Lucatello, S., Gratton, R., Cohen, J. G., Beers, T. C., Christlieb, N., Carretta, E., & Ramírez, S. 2003, AJ, 125, 875
Magain, P. 1984, A&A, 134, 189
Marigo, P., Girardi, L., Bressan, A., Groenewegen, M. A. T., Silva, L., & Granato, G. L. 2008, A&A, 482, 883
Marino, A. F., Piotto, G., Gratton, R., Milone, A. P., Zoccali, M., Bedin, L. R., Villanova, S., & Bellini, A. 2010, IAU Symposium, 268, 183
Martin, G.A., Fuhr, J.R., and Wiese, W.L. 1988, J.Phys.Chem.Ref.Data 17, Suppl. 3
McWilliam, A. 1997, ARA&A, 35, 503
Meylan, G., Mayor, M., Duquennoy, A., & Dubath, P. 1995, A&A, 303, 761
Mucciarelli, A., A&A, submitted
Norris, J. E., & Da Costa, G. S. 1995, ApJ, 447, 680
Norris, J. E., Freeman, K. C., & Mighell, K. J. 1996, ApJ, 462, 241
Norris, J. E. 2004, ApJ, 612, L25
Pancino, E., Ferraro, F. R., Bellazzini, M., Piotto, G., & Zoccali, M. 2000, ApJ, 534, L83
Pancino, E., Pasquini, L., Hill, V., Ferraro, F. R., & Bellazzini, M. 2002, ApJ, 568, L101
Pancino, E. 2003, Ph.D. Thesis, Bologna University, Italy
Pancino, E., Galfo, A., Ferraro, F. R., & Bellazzini, M. 2007, ApJ, 661, L155
Pancino, E., Carrera, R., Rossetti, E., & Gallart, C. 2010, A&A, 511, A56
Pietrinferni, A., Cassisi, S., Salaris, M., & Castelli, F. 2006, ApJ, 642, 797
Piotto, G., et al. 2005, ApJ, 621, 777
Piotto, G., et al. 2007, ApJ, 661, L53
Renzini, A. 2008, MNRAS, 391, 354
Rey, S.-C., Lee, Y.-W., Ree, C. H., Joo, J.-M., Sohn, Y.-J., & Walker, A. R. 2004, AJ, 127, 958
Romano, D., & Matteucci, F. 2007, MNRAS, 378, L59
Rutten, R. J., van der Zalm, E. B. J. 1984, A&AS, 55, 171
Salaris, M., Chieffi, A., & Straniero, O. 1993, ApJ, 414, 580
Sbordone, L., Bonifacio, P., Castelli, F., and Kurucz, R. L. 2004, Memorie della Società Astronomica Italiana Supplementi, 5, 93
Smith, V. V., Suntzeff, N. B., Cunha, K., Gallino, R., Busso, M., Lambert, D. L., & Straniero, O. 2000, AJ, 119, 1239
Shchukina, N. G., Trujillo Bueno, J., & Asplund, M. 2005, ApJ, 618, 939
Sneden, C. 1973, ApJ, 184, 839
Sollima, A., Ferraro, F. R., Pancino, E., & Bellazzini, M. 2005, MNRAS, 357, 265
Sollima, A., Pancino, E., Ferraro, F. R., Bellazzini, M., Straniero, O., & Pasquini, L. 2005, ApJ, 634, 332
Spite, M. 1967, Annales d'Astrophysique, 30, 685 Cohen, J. G. 2003, AJ, 125, 224
Spite, M., et al. 2005, A&A, 430, 655
Stanford, L. M., Da Costa, G. S., Norris, J. E., & Cannon, R. D. 2006, ApJ, 647, 1075
Starkenburg, E., et al. 2010, A&A, 513, A34
Stetson, P. B., & Pancino, E. 2008, PASP, 120, 1332
Suntzeff, N. B., & Kraft, R. P. 1996, AJ, 111, 1913
Thévenin, F., & Idiart, T. P. 1999, ApJ, 521, 753
van Leeuwen, F., Le Poole, R. S., Reijns, R. A., Freeman, K. C., & de Zeeuw, P. T. 2000, A&A, 360, 472
van Leeuwen, F., Hughes, J. D., & Piotto, G. 2002, Omega Centauri, A Unique Window into Astrophysics, 265,
Vanture, A. D., Wallerstein, G., & Brown, J. A. 1994, PASP, 106, 835
Vidal, C. R., Cooper, J., & Smith, E. W. 1973, ApJS, 25, 37
Villanova, S., et al. 2007, ApJ, 663, 296
Villanova, S., Carraro, G., Scarpa, R., & Marconi, G. 2010, New A, 15, 520